International Journal of Mechanical and Production Engineering Research and Development (IJMPERD)
ISSN(P): 2249-6890; ISSN(E): 2249-8001
Vol. 9, Issue 3, Jun 2019, 1259-1274

TRANS STELLAR • Journal Publications • Research Consultancy

Original Article

THE NUMERICAL ANALYSIS OF BUBBLE GROWTH AND BUBBLE FREQUENCY IN NUCLEATE BOILING USING NANOFLUIDS

K. V. NARASIMHA RAO[1*], K. AYYAPPA SWAMY[2] & VINAY ATGUR[3]

[1]*Professor, Department of Mechanical Engineering, Koneru Lakshmaiah Education Foundation (KLEF), Andhra Pradesh, India*

[2]*Student, Department of Mechanical Engineering, Koneru Lakshmaiah Education Foundation (KLEF), Vaddeswaram, Guntur District, Andhra Pradesh, India*

[3]*Assistant Professor, Department of Mechanical Engineering, KLEF, Andhra Pradesh, India*

ABSTRACT

The nucleate boiling phenomena is analysed for TiO_2 and Al_2O_3 aqueous Nanofluids using computational fluid dynamics. The use Nanofluid as a working fluid significantly enhances the boiling critical heat flux (CHF). It has been found that the CHF enhancement in boiling is dependent on the type of Nanofluid as well as its concentration. The present study observed that by increasing the nanoparticles concentration, the bubble frequency increases. Two sets of Nanofluids, viz. Al_2O_3 and TiO_2 with Volume of Fraction (VOF) of 0.05, 0.1, and 0.15 have been considered for the study. The obtained simulation results show that by increasing the nanoparticles concentration, the TSHF and HTC increase proportionally. TiO_2 nanoparticles with various VOF give better results after a time interval of 1.4 s compared to Al_2O_3 and water.

KEYWORDS: Nanofluids, Heat Transfer Coefficient, Total Surface Heat Flux, Critical Heat Flux & Concentration

Received: Apr 21, 2019; **Accepted:** May 11, 2019; **Published:** May 30, 2019; **Paper Id.:** IJMPERDJUN2019132

NOMENCLATURE

φ = Particles volume concentration

ρ_f = Density of the base fluid, kg/m^3

ρ_p = Density of the Nanoparticles, kg/m^3

μ_{nf} = Nanofluid viscosity, kg/ms

μ_{bf} = Water viscosity, kg/ms

c_{pnf} = Heat capacity of the Nanofluid, J/kg˚C

c_{pbf} = Heat capacity of the base fluid, J/kg˚C

c_{pp} = Heat capacity of the Nanoparticles, J/kg˚C

k_p = Thermal conductivity of the Nanoparticle, W/m˚C

k_{bf} = Thermal conductivity of the water, W/m˚C

φ_p = Volume fraction

Pe = Peclet number

Re = Reynolds number

Pr = Prandtl number

ABBREVIATIONS

VOF = Volume of Fraction

HTC = Heat Transfer Coefficient

TSHF = Total Surface Heat Flux

INTRODUCTION

Boiling heat transfer plays an important role in a variety of industrial process and applications like refrigeration, heat exchangers, cooling of electronic components and power generation. Boiling heat transfer enhancement process is vital and could make a significant impact on the industrial growth.

Nanofluids are one of the new kind of heat Transfer fluids in which Nano meter sized particles are dispersed uniformly. Recently many researchers have proposed a new approach that will considerably enhance the boiling phenomena. In the study of boiling regimes, nucleate boiling is an efficient heat transfer mechanism. However, critical heat flux (CHF) phenomenon is the thermal limit during the heat transfer phase change where heat transfer is maximized followed by drastic degradation. The study of bubble nucleation, growth and detachment are inherently complex phenomena, characterized by formation of vapour bubbles on heated wall. Numerical simulation for analysing the bubble dynamics and heat transfer in nucleate boiling has been studied by several investigators [1-7]. Recently, numerical studies have been carried out for analysing bubble dynamics and heat transfer on a horizontal surface. Use of Nanofluids play a key role in improving the process efficiency, increasing the CHF and reducing the operating cost; this is where Nanofluids emerged as efficient heat transfer fluids. Research on enhancement of CHF using Nanofluid under convective flow condition has also been studied, but to a lesser extent. Interestingly majority of the experimental data are on the effect of Nanofluid on the CHF. There is a significant gap in the study of bubble nucleation and detachment which also plays a vital role in studying the heat transfer applications. The main advantage of using Nanofluid for the heat transfer applications is the ability of the Nanofluids to alter these properties like thermal conductivity, specific heat, density, surface wettability. These properties can be adjusted by varying the Nanoparticles concentrations in the base fluid.

In the present work, two metal oxides - Nanoparticles Al_2O and TiO_2 are considered for the analysis, which are suspended in water. Numerical simulation has been carried out for analysing the bubble dynamics, bubble detaching frequency, surface critical heat flux and heat transfer coefficient and the results are compared with water under transient condition. Kim and Kim (2009) [1] reported that Nanoparticle motion depends on hydrodynamic forces formed around the surface, which lead to disappearance of influence of Nanoparticle and completely depend upon the volume concentration (vol %). They conducted experiments on nucleate boiling using different TiO_2, Al_2O_3 Nanofluids and stated the enhancement of CHF up to 100% when compared with water. They stated the reason as deposition of oxides of Nanoparticles coated on heater surface, which improves the wettability, which in turn enhances CHF. Experimental investigations were conducted by You et al. [2] on a flat square plate heater placed in Nanofluid with a fine proportion of Nanoparticles mixed and observed enhancement of CHF.

Li (2016) [3] conducted CFD analysis, observed velocity vector contours and stated that the vapour velocity during the departure is much more than the vapour velocity during the growth of bubble. He has shown the Eddies

formation and flow pattern of liquid around the bubble and inside the bubble. Buongiorno and Hu (2010) [4] after conducting experimental investigations have observed the Enhancement of CHF by Nanofluid where nucleate boiling takes place. They also stated the incremental CHF for both Al_2O_3 and SiO_2 of 200% and 60% respectively for a small proportion Nano particle dispersed in water and compared with water.

Wei et al. (2015) [5] found that the effect of growing diameter is inversely proportional to gravity. They came to the conclusion using the thermal lattice-Boltzmann method and correlation between the departure diameter and the gravity. The bubble diameter at the time of departure is given by:

$$D_d = \theta_w \sqrt{\frac{\sigma}{g(\rho_l - \rho_v)}}$$

After conducting both experimental and CFD analysis on pool boiling by taking a heated wire, using Nanofluid as fluid domain Girish Sapre et al. (2018) [6] concluded TiO_2 has a high bubble frequency compared with Al_2O_3 which result increase in HTC and TSHF. After theoretical study author Narendra et al. (2018) [7] has observed that Nanofluid thermal conductivity increases with increase in volume concentration of nanoparticles, comparing the thermal conductivity of both TiO_2 and Al_2O_3 Nanofluid concluded TiO_2 has high thermal conductivity then Al_2O_3. ANSYS Fluent software package has been utilized to solve many thermal engineering problems successfully and many of the results are found to be reasonably in good agreement with test data [8-11]. Base fluid as well as NanoFluids characteristics have been examined in [12-16].

THERMO PHYSICAL PROPERTIES OF NANOFLUID

Akilu et al. (2016) [17] has given the correlation for obtaining thermo-physical properties for Nanofluids after considering all the parameters like VOF, particle size and shape of the nano particles. Koca et al. (2018) [18] has stated the effect of nano particle size on the viscosity of Nanofluid, which will affect the bubble growth and bubble frequency. The following equations are used to calculate the properties of Nanofluids.

- $\rho_{nf=(1-\varphi)\rho_{bf+}\varphi\rho_p}$

  Where;

  ρ_{nf} = Density of the Nanofluid, kg/m^3

  φ = Particles volume concentration

  $\rho_{f=}$ Density of the base fluid, kg/m^3

  $\rho_{p=}$ Density of the Nanoparticles, kg/m^3

- $\mu_{nf} = (1 + 2.5\varphi)\mu_{bf}$

Where;

μ_{nf} = Nanofluid viscosity, kg/ms

μ_{bf}= Water viscosity, kg/ms

- $c_{p_{nf}} = \frac{(1-\varphi)\rho_{bf} c_{p_{bf}} + \varphi \rho_p c_{p_p}}{\rho_{nf}}$

Where;

c_{pnf} = Heat capacity of the Nanofluid, J/kg˚C

c_{pbf}= Heat capacity of the base fluid, J/kg˚C

c_{pp}= Heat capacity of the Nanoparticles, J/kg˚C

- $k_{eff} = \frac{k_p + 2k_{bf} + 2(k_p - k_{bf})\varphi_p}{k_p + 2k_{bf} - (k_p - k_{bf})\varphi_p} k_{bf}$

Where;

k_p= Thermal conductivity of the Nanoparticle, W/m˚C

k_{bf}= Thermal conductivity of the water, W/m˚C

φ_p= Volume fraction

- $Nu = 0.4328\ (1+11.285\varphi^{0.754} Pe^{0.218}) Re^{0.333} Pr^{0.4}$

Where,

φ = Volume fraction

Pe = Peclet number

Re = Reynolds number

Pr = Prandtl number

Following tables [1-3] give the calculated property values of different Nanofluids:

Table 1: Properties of Al_2O_3-Water Nanofluid

Al_2O_3-Water				
Volume Fraction	**Density [kg/m^3]**	**Cp [J/kg-K]**	**μ [kg/m-s]**	**K [W/m-K]**
0.05	1145.745	3589.25	9.585E-4	0.70514
0.1	1294.39	3134.965	1.065E-3	0.807006
0.15	1443.035	2774.264	1.1715E-3	0.9202

Table 2: Properties of TiO_2-Water Nanofluid

TiO_2-Water				
Volume Fraction	**Density [kg/m^3]**	**Cp [J/kg-K]**	**μ [kg/m-s]**	**K [W/m-K]**
0.05	1147.24	3574.421	9.525E-4	0.6904
0.1	1297.39	3109.776	1.065E-3	0.7748
0.15	1447.535	3036.229	1.1715E-3	0.86696

Table 3: Properties of Water

Water			
Density [kg/m^3]	**Cp [J/kg-K]**	**μ [kg/m-s]**	**K [W/m-K]**
998.2	4182	0.6	0.001003

COMPUTATIONAL DOMAIN

A rectangular section of 0.004m*0.008m computational domain is set up for bubble capture, resembling a cylindrical vessel taken in 2D.

MESH METHOD

Grid Independence studies have been conducted to acquire consistent, accurate and reliable results. It is observed that the number of elements and nodes kept on increasing until the heat transfer coefficient (HTC) of water became stable. The summary of numerical experiments conducted for deciding the grid size has been tabulated below (Table 5). A graph is also plotted to show the grid independence.

Table 4: Results of Grid Independence Studies

No. of Elements	Heat Transfer Coefficient of Water at 0.2 s
14323	1.842
16201	1.876
18822	1.985
20301	2.030
20811	2.029
30242	2.031

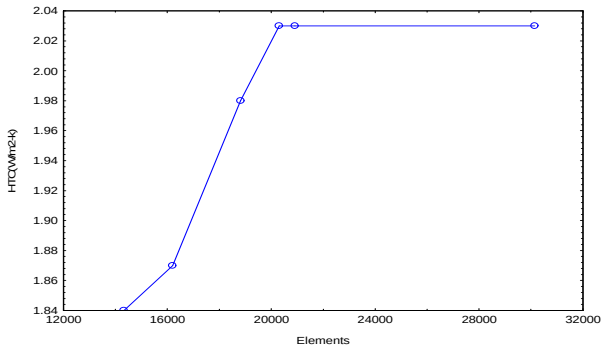

Figure 1

Based on the above numerical experiments conducted and to maintain less computation time and space, the number of elements has been fixed at 20301 and the number of nodes at 20,000. The mesh has been generated by using ICEM CFD (meshing tool).

Figure 2 represents the mesh and boundary conductions and exponential grid spacing.

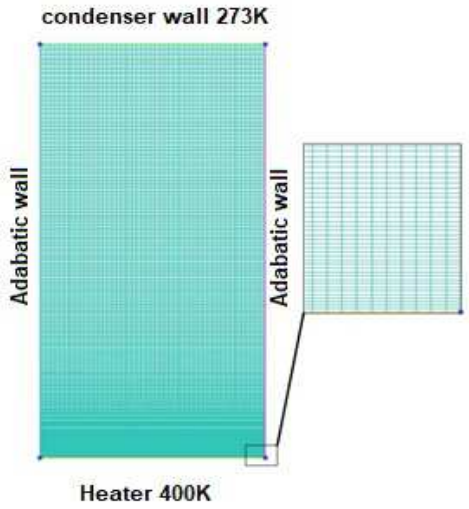

Figure 2: Exponential Gird with Representation of Boundary Conductions

Micro level Spacing of 0.0001 mm is given at the heater surface to capture the bubble dynamics and bubble departure. Bi-exponential grid ratio is given as 1.5 as shown in Figure 1.

GOVERNING EQUATIONS

The analysis is based on transient, two-phase, three-dimensional, turbulent flow with the Boussinesq approximation for the buoyancy term and VOF model for capturing the bubble dynamics under multi-phase. The governing equations run in the background of the software interface; these equations describe continuity, momentum and energy transport. The following governing equations are used in computation fluid dynamics Xiaobin et al. (2015) [19].

Continuity Equation

$$\frac{\partial}{\partial t}(\alpha_q \rho_q) + \nabla(\alpha_q \rho_q v_q) \tag{1}$$

P = Liquid phase

Q = Vapour phase

α- = Volume fraction

v_q = Velocity of phase q (vapour)

Momentum Equation

$$\frac{\partial}{\partial t}\left(\alpha_q \rho_q \vec{v_q}\right) + \nabla\left(\alpha_q \rho_q \vec{v_q}\vec{v_q}\right) = -\alpha\nabla P + \nabla\bar{\bar{\tau}} + \alpha_q \rho_q \vec{g} + \vec{R_{pq}} + \left(\vec{F_{lift}} + \vec{F_{td,q}}\right) \tag{2}$$

Energy Equation

$$\frac{\partial}{\partial t}\left(\alpha_q \rho_q h_q\right) + \nabla\left(\alpha_q \rho_q \vec{u_q} h_q\right) = \alpha_q \frac{dP}{dt} + \bar{\bar{\tau}}\nabla\vec{u_q} - \nabla\dot{q}_q + \sum_{p=1}^{n} Q_{pq} \tag{3}$$

BOUNDARY CONDITIONS

Bottom edge as heater is provided with a constant temperature of 400 K, top edge as condenser wall is provided with a constant temperature of 273 K, remaining edges are set adiabatic conditions.

RESULTS AND DISCUSSION

Initial bubble growth and departure time are numerically investigated in this investigation. Horizontal heating is applied to the bottom wall surface by maintaining a constant temperature of 400 K. Similarly, top wall is kept at a constant temperature of 273 K (Condensation condition) and the other walls are given adiabatic conditions.

To observe the bubble growth and bubble dynamics, small time step of 1×10^{-5} s is taken during numerical simulation. Hence, simulated initial bubble along with time is observed from image obtained from Numerical study for water, Al_2O_3-Water Nanofluid and TiO_2-Water Nanofluid at three different VOFs of 0.05, 0.1 and 0.15 [Figures 2-4c].

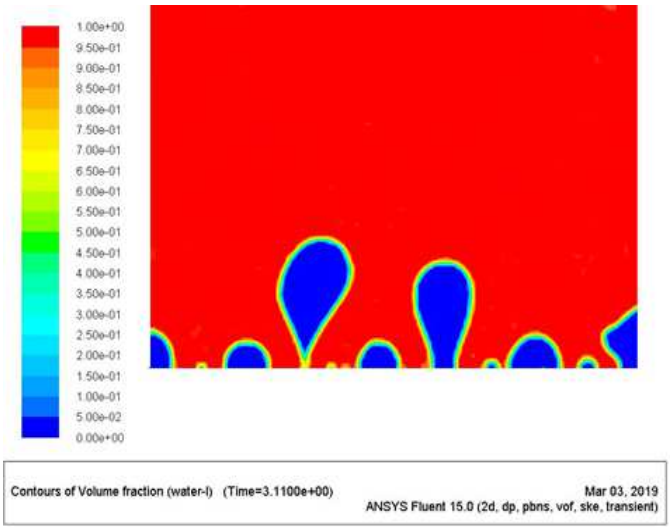

Figure 2: Phase Contour for Water During Bubble Departure (Red Colour Represents the Liquid Phase and the Blue Represents the Vapour Phase)

In Figure 2 indicates the bubble growth and detachment in a heated surface simulation of the bubble detachment has been carried out at the centre of the compaction demine as time evolves the bubbles gradually groups from the heated surface and it will moves upwards due to gravity and the density difference there by bubble experiences an upward force leading to its shape deformation and lift off takes place from the wall surface Xu et al. (2018) [20]. As the bubble moves away from the wall its shape deforms again due the unbalance action caused by bouncy and viscous drag force from the surrounding liquid.

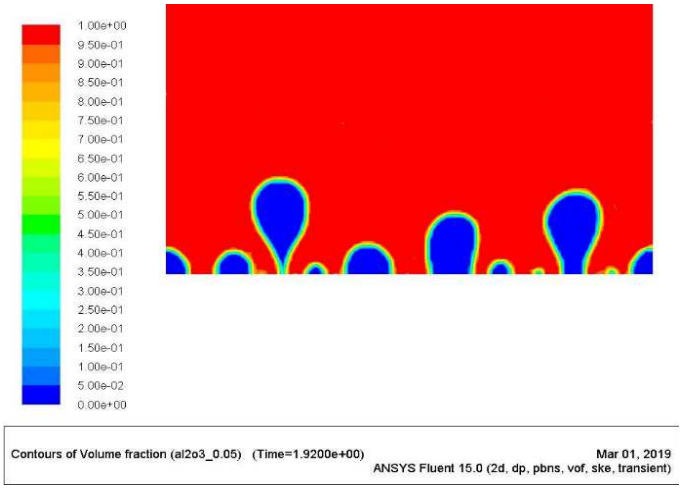

Figure 3a: Phase Contour for Al_2O_3-Water Nanofluid with a VOF of 0.05 During Bubble Departure (Red Colour Represents the Liquid Phase and the Blue Represents the Vapour Phase)

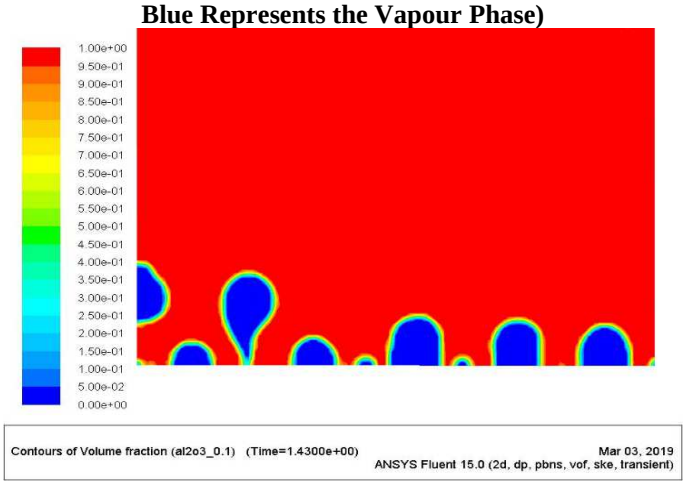

Figure 3b: Phase Contour for Al_2O_3-Water Nanofluid with a VOF of 0.1 During Bubble Departure (Red Colour Represents the Liquid Phase and the Blue Represents the Vapour Phase)

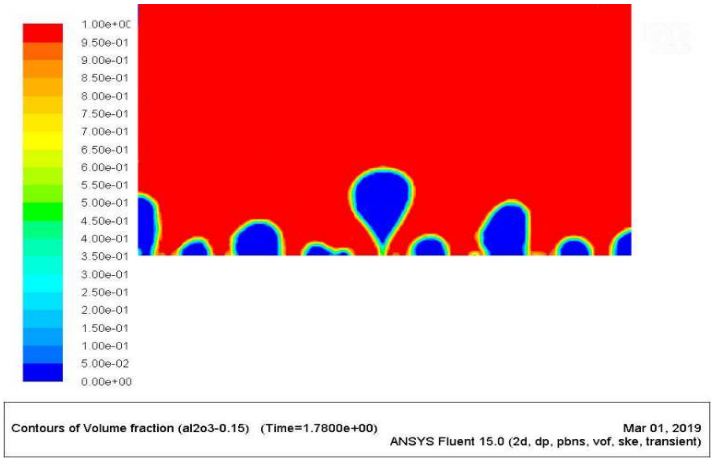

Figure 3c: Phase Contour for Al_2O_3-Water Nanofluid with a VOF of 0.15 during Bubble Departure (Red Colour Represents the Liquid Phase and the Blue Represents the Vapour Phase)

Figure 3a indicates the bubble formation and departure for the Al_2O_3 Nanofluid with 0.05 VOF and Figures 3b and 3c indicate bubbles formation and departure for the same Nanofluid and with 0.1 and 0.15 VOF. In all the three figures

we can observe that by increasing the percentage of Nanoparticles heat flux increases and bubble departures from surface with a time gap and the waiting time for the formation of the new bubble decreases, it means by increasing volume concentration the bubbles form rapidly from the heated surface [21-22]. By increasing volume concentration the bubble lift of diameter decreases steeply due to increase of the heat flux.

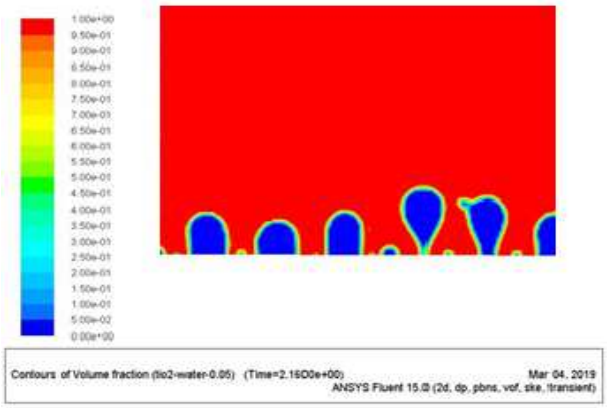

Figure 4a: Phase Contour for TiO_2-Water Nanofluid with a VOF of 0.05 during Bubble Departure (Red Colour Represents the Liquid Phase and the Blue Represents the Vapour Phase)

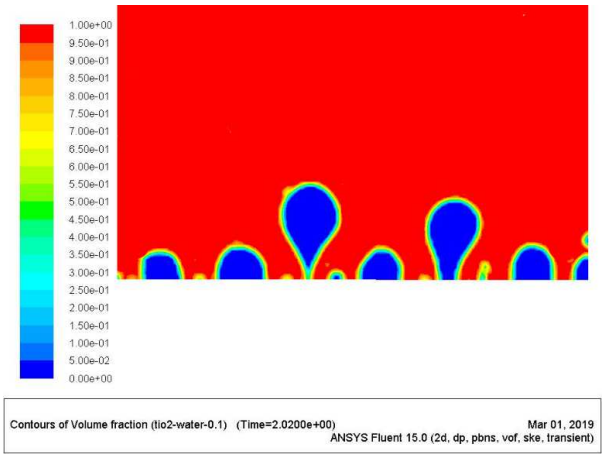

Figure 4b: Phase Contour for TiO_2-Water Nanofluid with a VOF of 0.1 during Bubble Departure (Red Colour Represents the Liquid Phase and the Blue Represents the Vapour Phase)

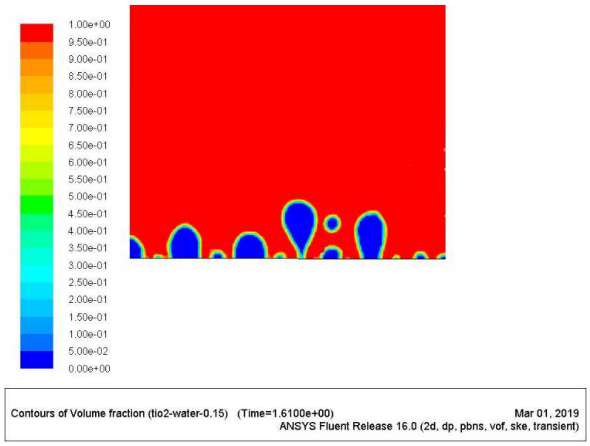

Figure 4c: Phase Contour for TiO_2-Water Nanofluid with a VOF of 0.15 during Bubble Departure (Red Colour Represents the Liquid Phase and the Blue Represents the Vapour Phase)

Figures 4a, 4b, 4c indicate the bubble formation and departure from the heated surface for the TiO_2 Nanofluid for 0.05, 0.1, 0.15 volume concentration. While comparing the thermal properties of Al_2O_3 and TiO_2 mono fluids it has been observed that the thermal conductivity is higher for the Al_2O_3 Nanofluids, therefore we can observe a good number of bubbles in Al_2O_3 Nanofluids Li et al. (2016) [23]. Whereas the bubble frequency is more for tio2 it means the consecutive bubble formation will be more in the TiO_2 Nanoparticles due to the lesser specific heat capacity compared to the Al_2O_3 Nanofluids. The bubble departure is a function of the gravity force which is proportional to the $g^{0.5}$; it means initial bubble radius influences the path of the early growth period which is going to reflect in the simulation for a great departure. Figure 5 shows bubble dynamics and growth of bubble and detachment of bubble from the heated surface. Time steps are also provided.

Table 5

0.9(s)	1.1(s)	1.2(s)	1.3(s)	1.4(s)	1.59(s)	1.7(s)	1.8(s)

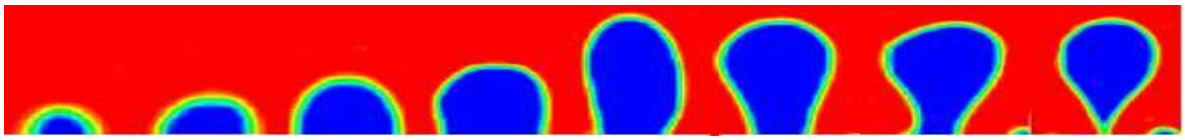

Figure 5: Phase Contour of Development of Bubble and Departure of Bubble form Surface for Al_2O_3 of VOF of 0.1

The following bubble growth and departure shown in the figure is compared with the results obtained by the author Bang et al. (2005) [24], the departure time steps have been considered.

Nanofluids with 0.05% of alumina show similar TSHF when compared to 0.1% and 0.15% of concentration, due to the deposition of the Nano particle on the heater surface, which affects the boiling phenomena (CHU et al., 2011) [25]. Nanofluids used in the study have contributed to the enhancement of TSHF. Various researchers criticized that deposition of Nanoparticles on the surfaces is the main cause beyond the TSHF enhancement due to the effect of surface liquid wettability and morphology [26-27]. The phenomenon of wettability varies depending on the Nanoparticles concentration with the base fluid. In the pool boiling phenomena, TSHF varies with various concentration of Nano particles. At a concentration of 0.05, the critical heat flux for all the Nanofluids increase steeply (Suriyawong et al., 2013) [27]. By increasing the Nanoparticles concentration it has been observed that there is no sizable increase in the TSHF. All the Nanofluids seems to have the same characteristics of TSHF enhancement qualitatively (Ivey, 1967 and Kim et al., 2007) [28-29].

Figures 6 and 7 give the comparison of TSHF Vs HTC for Al_2O_3 and TiO_2 concentrations at different time intervals.

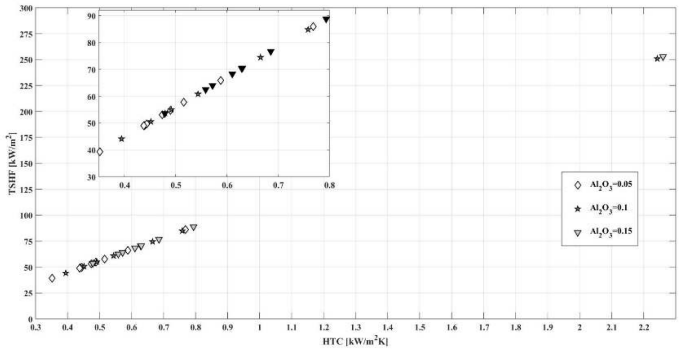

Figure 6: Comparison of HTC Vs. TSHF of Al_2O_3 (Vol% of 0.05, 0.1, 0.15)

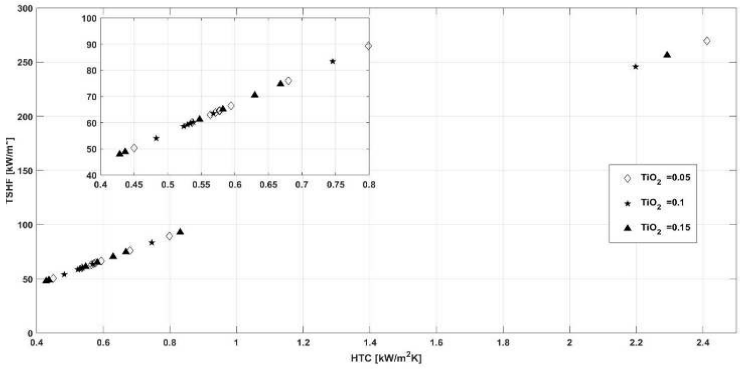

Figure 7: Comparison of HTC Vs. TSHF of TiO_2 (Vol% of 0.05, 0.1, 0.15)

As could be seen, there is a linear variation for all the Al_2O_3 and TiO_2 concentration. Suriyawong et al. (2013) [30] has also obtained similar results during their investigation with Al_2O_3-water Nanofluid.

Figure 8 shows fluctuation of HTC along with time on the heated surface when investigated and compared between Water, Al_2O_3-0.05, and TiO_2-0.05 Nanofluid.

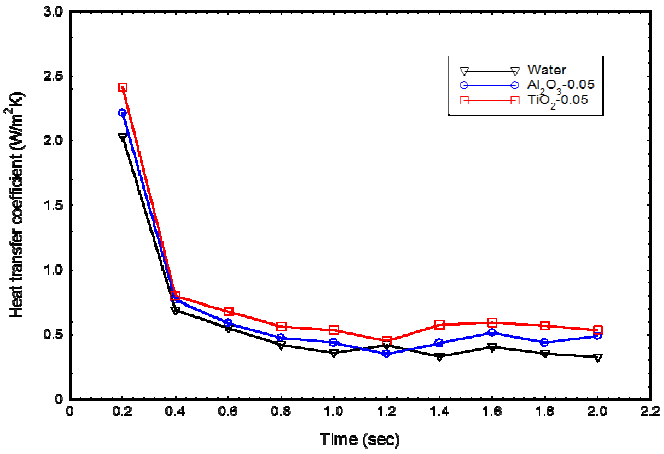

Figure 8: Comparison of HTC Vs. Time of Water, Al_2O_3-0.05, TiO_2-0.05

Figure 8 shows variation of HTC with respect to the bubble dynamics time. The graph shows that the HTC decreases between 0.2-0.4 s, and remains constant from 0.4 s onwards for TiO_2 Nanofluid with 0.05 concentration. As could be seen from the figure, higher heat transfer coefficients have been observed.

Due to the lesser c_p value of 3574.421 [J/kg-K], when compared to Al_2O_3 at 0.05 concentration 3589.25 [J/kg-K] from the property it has been observed that density of TiO_2 Nanofluid with 0.1 % concentration has a lesser value compared to Al_2O_3 due to this the bubble dynamics for the TiO_2 Nanofluids is efficient.

Figure 9 shows fluctuation of HTC along with time on the heated surface when investigated and compared between Water, Al_2O_3-0.1 and TiO_2-0.1 Nanofluids.

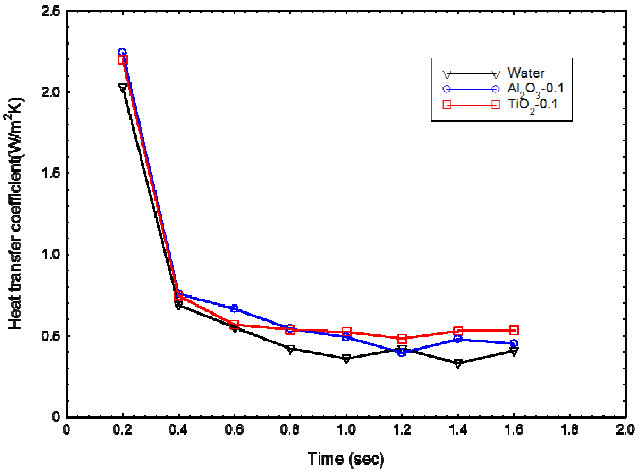

Figure 9: Comparison of HTC Vs. Time of Water, Al_2O_3-0.1, TiO_2-0.1

Figure 9 shows the HTC vs time for Al_2O_3 and TiO_2 Nanofluids for 0.1% of concentration, compared with the water. As can be observed that form a time period of 0.2 to 0.4 s, there is a sudden decrease in the HTC value and from 0.2 to 0.4 s and the HTC will remain nearly constant from 0.6 s onwards. This variation is captured in the contour plots and it has been observed that during 0.2-0.4 s, the convection current plays a significant role and the small bubbles raises from the surface and collapse due to the forces of buoyancy from the time period 0.6s onwards. It can also be seen that bubbles rise constantly throughout the structure in a uniform manner; therefore heat transfer coefficient will be nearly constant (Kamatchi et al., 2015) [31].

Figure 10 shows fluctuation of HTC along with time on the heated surface when investigated and compared between Water, Al_2O_3-0.15 and TiO_2-0.15 Nanofluids.

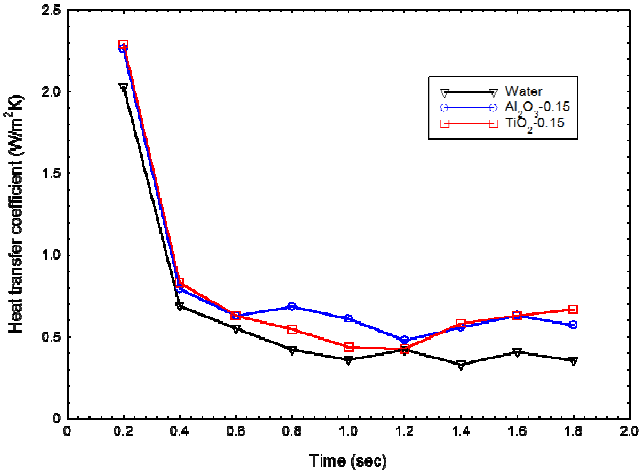

Figure 10: Comparison of HTC Vs. Time of Water, Al_2O_3-0.15, TiO_2-0.15

Figure 10 shows that for a time period up to 0.4 s the HTC decreases steeply for all the three fluids which can be claimed as in the time period between 0 to 0.4 s. The convection current plays an important role even though the bubbles raise and then will collapse at a shorter distance. From 0.4 s onwards, the bubble growth takes place repeatedly and the bubbles move from the surface freely and travel a longer distance. Since Al_2O_3 Nanofluid is having higher thermal conductivity compared to 0.1 and 0.5 VOF, it shows better HTC compared to TiO_2 from time period 1.2 s onwards there is a variation in the HTC for TiO_2 rather than Al_2O_3 due to the bubble density variation; the bubble raise will be rapid for the TiO_2 Nanofluid Kshirsagar et al. (2014) [32].

The following table gives the initial and the next preceding bubble departure time. The bubble waiting time which is the difference between the initial or first and the second bubble, which allow us to observe the time gap taken to form the next bubble. Later bubble frequency which is the inverse of bubble wait time is calculated. The results are presented in Table 5.

Table 6: Bubble Waiting Time (t_w) and Bubble Frequency (f)

Sl. No.	Fluid	Departure Time (s)	Second Bubble	Bubble Wait time(t_w)	Bubble Frequency (f) f = 1/ t_w
1	Water	3.11	3.37	0.26	3.8461
2	Al_2O_3-Water				
VOF	0.05	1.92	2.13	0.21	4.7619
	0.1	1.87	2.04	0.17	5.8823
	0.15	1.78	1.93	0.15	6.6666
3	TiO_2-Water				
VOF	0.05	1.97	2.16	0.19	5.2631
	0.1	1.62	1.77	0.15	6.6666
	0.15	1.61	1.74	0.13	7.6923

As it can be seen from the above values, can be concluded that higher the bubble frequency, lesser will the bubble waiting time which further implies better TSHF and HTC.

CONCLUSIONS

To analyse the bubble nucleation, growth and detachment from the plane, smooth, heated surface is carried out using CFD the boiling phenomena has been simulated by an Euler description of two-phase flow (volume of fraction model). The analysed bubble profile show a decrease in detachment of the bubble size and increase in frequency they will compact with each other for the thermal energy from the heated surface. CFD results confirm the potential of Euler two-phase flow for the boiling simulation which is useful to industrial applications. The studies concluded that by increasing the volume of fraction for Al_2O_3 and TiO_2 nanoparticles bubble frequency increases which can be confirmed by the obtained HTC values. The studies reviles that after some time of intervals TiO_2 Nanoparticles gives us the better heat transfer rate compared to the Al_2O_3, due to the increased in the bubble density TiO_2 VOF Nanofluid gives us the better results which can be confirmed by the thermal physical properties.

ACKNOWLEDGEMENTS

The Author would like to place on record the support received from Ms. R. Charulatha Madhuri, II M. Tech. Student, Dept. of Mechanical Engineering, KLEF (Deemed to be University) in carrying out this work.

REFERENCES

1. *Kim, H. and Kim, M. (2009). Experimental study on the characteristics and mechanism of pool boiling CHF enhancement using nano-fluids, Heat and Mass Transfer, May 2009, Vol 45, Issue 7, pp. 991-998, Springer.*
2. *You, S. M., Kim, J. H. and Kim, K. H. (2003). Effect of nanoparticles on critical heat flux of water in pool boiling heat transfer. Applied Physics Letters, 83 (16), 3374–3376. https://doi.org/10.1063/1.1619206.*
3. *Li, D. (2016). Preparation and properties of copper oil based nanofluids, 6 (1), 1–17. https://doi.org/10.1186/1556.*
4. *Buongiorno, J., and Hu, L. (2010). Nanofluid Heat Transfer Enhancement for Nuclear Reactor Applications, 517–522. https://doi.org/10.1115/mnhmt2009-18062*
5. *Wei, Y., Feng, K., & Li, Q. (2015). Numerical Simulations of a Bubble Growth and Departure on the Horizontal Wall Using Thermal Lattice Boltzmann Method. The Journal of Computational Multiphase Flows, 7(2), 111–116. https://doi.org/10.1260/1757-482x.7.2.111*
6. *Girish Sapre et al. (2018). CFD Analysis on Bubble Growth and Bubble Departure in Pool Boiling. International Journal of Mechanical and Production Engineering Research and Development, 8 (2), 671–676. https://doi.org/10.24247/ijmperdapr201878*
7. *Nerusu Narendra and K. V. Narasimha Rao. (2018). Experimental Evaluation of Performance of Air-Conditioning Compressor Due To Al2O3 Nanoparticles in Lubricating Oil. International Journal of Mechanical and Production Engineering Research and Development (IJMPERD), 8 (3), 603–614. https://doi.org/10.24247/ijmperdjun201865*
8. *Konda, J. R., Madhusudhana, N. P. and Konijeti, R. (2018). MHD mixed convection flow of radiating and 8-chemically reactive Casson nanofluid over a nonlinear permeable stretching sheet with viscous dissipation and heat source. Multidiscipline Modelling in Materials and Structures, 14 (3), 609–630. https://doi.org/10.1108/MMMS-10-2017-0127*
9. *Saktivel M. (2018). Fluent Analysis of shell and Tube heat Exchanger Using Nanofluid. 9(4), 185–191.*
10. *Koundinya, V. K. (2017). Computational Analysis of Propellant Flow on the Structure of The Wall of A Bi-Propellant Thruster. 8(5), 607–620.*
11. *Teja, G. V., District, G. and District, G. (2017). Numerical Investigation on Heat Transfer And Fluid Flow of Shell-Side For Shell And Tube Heat Exchanger With Hexagonal Vent Baffle By Using. 8 (5), 995–1009.*
12. *Narendra, G. and Kumar, S. (2019). Modelling and Analysis of Kaplan Turbine Blade Using CFD. (January).*
13. *Janjanam, N., Babu, K. R., Chowhan, S. S., Khan, A. and Teja, M. (2017). Comparison of Naca 23024 Aerofoil with And Without Vortex Generators Using. 8(5), 556–566.*
14. *Sandeep, G. (2017). Karanja Oil as an Alternative Fuel with Air Preheater. 8 (5), 218–225.*
15. *Jagadishwar, K. and Babu, S. S. (2017). Performance Investigation of Water and Propylene Glycol Mixture Based Nano-Fluids on Automotive Radiator for Enhancement of Heat Transfer. 8 (7), 822–833.*
16. *Prathyusha, B. G. R., Naveen Janjanam, Narasimha Rao, K. V. and Sandeep, G., Numerical Investigation on Shell & Tube Heat Exchanger with Segmental and Helix Baffles, International Journal of Mechanical and Production Engineering Research and Development (IJMPERD), Vol. 8, Issue 3, June 2018, pp. 183-192. https://doi.org/10.24247/ijmperdjun201821*
17. *Akilu, S., Sharma, K. V., Baheta, A. T and Mamat, R. (2016). A review of thermo-physical properties of water based composite nanofluids. Renewable and Sustainable Energy Reviews, 66, 654–678. https://doi.org/10.1016/j.rser.2016.08.036*

18. *Koca, H. D., Doganay, S., Turgut, A., Tavman, I. H., Saidur, R. and Mahbubul, I. M. (2018). Effect of particle size on the viscosity of nanofluids: A review. Renewable and Sustainable Energy Reviews, 82 (July 2017), 1664–1674. https://doi.org/10.1016/j.rser.2017.07.016*

19. *Xiaobin, Z., Wei, X., Jianye, C., Yuchen, W. and Tang, K. (2015). CFD simulations and experimental verification on nucleate pool boiling of liquid nitrogen. Physics Procedia, 67, 569–575. https://doi.org/10.1016/j.phpro.2015.06.077*

20. *Thakur, G., & Singh, G. Experimental Investigation Of Heat Transfer Characteristics In Al2o3–Water Based Nanofluids Operated Shell And Tube Heat Exchanger With Air Bubble Injection.*

21. *Xu, J., Zhao, D., Bi, J., Christopher, D. M. and Huang, Y. (2018). Numerical study of bubble growth and merger characteristics during nucleate boiling. Progress in Nuclear Energy, 112(December 2017), 7–19.*

22. *Liang, G. and Mudawar, I. (2018). Review of pool boiling enhancement with additives and nanofluids. International Journal of Heat and Mass Transfer, 124, 423–453. https://doi.org/10.1016/j.ijheatmasstransfer.2018.03.046*

23. *Wu, J. M., & Zhao, J. (2013). A review of nanofluid heat transfer and critical heat flux enhancement - Research gap to engineering application. Progress in Nuclear Energy, 66, 13–24. https://doi.org/10.1016/j.pnucene.2013.03.009*

24. *Li, D. (2016). Publisher main menu Preparation and properties of copper oil based nanofluids. 6(1), 1–17.*

    https://doi.org/10.1186/1556

25. *Bang, I. C., & Heung Chang, S. (2005). Boiling heat transfer performance and phenomena of Al2O 3-water nano-fluids from a plain surface in a pool. International Journal of Heat and Mass Transfer, 48(12), 2407–2419.*

    https://doi.org/10.1016/j.ijheatmasstransfer.2004.12.047

26. *CHU, I.-C., NO, H. C., & SONG, C.-H. (2011). Bubble Lift-off Diameter and Nucleation Frequency in Vertical Subcooled Boiling Flow. Journal of Nuclear Science and Technology, 48(6), 936–949. https://doi.org/10.3327/jnst.48.936*

27. *Wongcharee, K., & Eiamsa-ard, S. (2012). Heat transfer enhancement by using CuO/water nanofluid in corrugated tube equipped with twisted tape. International Communications in Heat and Mass Transfer, 39(2), 251-257.*

28. *Wang, X., Wu, Z., Wei, J. and Sundén, B. (2019). Correlations for prediction of the bubble departure radius on smooth flat surface during nucleate pool boiling. International Journal of Heat and Mass Transfer, 132, 699–714.*

    https://doi.org/10.1016/j.ijheatmasstransfer.2018.12.029

29. *Suriyawong, A., Dalkiliç, A. S. and Wong wises, S. (2013). Nucleate Pool Boiling Heat Transfer Correlation for TiO_2-Water Nanofluids. Nanofluids, 9(5), 171–188. https://doi.org/10.1520/stp156720120011*

30. *Ivey, H. J. (1967). Relationships between bubble frequencies, departure diameter and rise velocity in nucleate boiling. International Journal of Heat and Mass Transfer, 10(8), 1023–1040. https://doi.org/10.1016/0017-9310(67)90118-4*

31. *Kim, H. D., Kim, J. and Kim, M. H. (2007). Experimental studies on CHF characteristics of nano-fluids at pool boiling. International Journal of Multiphase Flow, 33(7), 691–706. https://doi.org/10.1016/j.ijmultiphaseflow.2007.02.007*

32. *Suriyawong, A. and Wong wises, S. (2010). Nucleate pool boiling heat transfer characteristics of TiO2-water nanofluids at very low concentrations. Experimental Thermal and Fluid Science, 34(8), 992–999.*

    https://doi.org/10.1016/j.expthermflusci.2010.03.002

33. *Kamatchi, R. and Venkatachalapathy, S. (2015). Parametric study of pool boiling heat transfer with nanofluids for the enhancement of critical heat flux: A review. International Journal of Thermal Sciences, 87, 228–240.*

    https://doi.org/10.1155/2012/435873

34. *Kshirsagar, J. M. and Shrivastava, R. (2014). Review of the influence of nanoparticles on thermal conductivity, nucleate pool boiling and critical heat flux. Heat and Mass Transfer/Warme- Und Stoffubertragung, 51(3), 381–398.*

    https://doi.org/10.1007/s00231-014-1412-3.